Climp-63-mediated binding of microtubules to the ER affects the lateral mobility of translocon complexes

Andrei V. Nikonov[1], Hans-Peter Hauri[2], Brett Lauring[3] and Gert Kreibich[1,*]

[1]Department of Cell Biology, New York University School of Medicine, New York, NY 10016, USA
[2]Biozentrum, University of Basel, CH-4056, Basel, Switzerland
[3]Department of Pathology, College of Physicians and Surgeons, Columbia University, New York, NY 10032, USA
*Author for correspondence (e-mail: kreibg01@popmail.med.nyu.edu)

Accepted 27 April 2007
Journal of Cell Science 120, 2248-2258 Published by The Company of Biologists 2007
doi:10.1242/jcs.008979

Summary

Microtubules are frequently seen in close proximity to membranes of the endoplasmic reticulum (ER), and the membrane protein CLIMP-63 is thought to mediate specific interaction between these two structures. It was, therefore, of interest to investigate whether these microtubules are in fact responsible for the highly restricted lateral mobility of the translocon complexes in M3/18 cells as described before. As determined by fluorescence recovery after photobleaching, the breakdown of microtubules caused by drug treatment or by overexpression of the microtubule-severing protein spastin, resulted in an increased lateral mobility of the translocons that are assembled into polysomes. Also, the expression of a CLIMP-63 mutant lacking the microtubule-binding domain resulted in a significant increase of the lateral mobility of the translocon complexes. The most striking increase in the diffusion rate of the translocon complexes was observed in M3/18 cells transfected with a siRNA that effectively knocked down the expression of the endogenous CLIMP-63. It appears, therefore, that interaction of microtubules with the ER results in the immobilization of translocon complexes that are part of membrane-bound polysomes, and may play a role in the mechanism that segregates the rough and smooth domains of the ER.

Key words: Endoplasmic reticulum, Translocon complexes, Microtubules, FRAP, CLIMP-63

Introduction

The fluid mosaic membrane model that was proposed about 30 years ago emphasized the free mobility of membrane proteins in the plane of the membrane (Singer and Nicolson, 1972). Since then, it was found that many membrane proteins are not completely free to diffuse in the plane of the lipid bilayer. They may be retarded in their lateral diffusion or completely immobilized through interactions with cytoskeletal elements, with extracellular matrix proteins, or by becoming a part of large oligomeric arrays. These insights were gained, at least in part, through biophysical methods, including fluorescence recovery after photobleaching (FRAP) (Jacobson et al., 1995; Lippincott-Schwartz et al., 2001). The rate of fluorescence recovery can be used to calculate an effective diffusion constant (D_{eff}) for the mobile fraction of the GFP-tagged structure (Lippincott-Schwartz et al., 1999), because the diffusion of integral membrane proteins in the lipid bilayer decreases with the natural logarithm of the radius of the diffusing molecule (Marguet et al., 1999; Vaz et al., 1982). Incomplete recovery indicates the presence of an immobilized fraction of the tagged molecules.

The rough endoplasmic reticulum (ER) is the site where transmembrane or secretory proteins are made on polysomes attached to ER membranes. The attachment of individual ribosomes to the ER membrane is mediated by a complex molecular apparatus with Sec61p at its core (Clemons, et al., 2004; Gilmore, 1993; Rapoport et al., 1996), that effects the signal sequence-mediated targeting, co-translational translocation and processing of nascent polypeptide chains (Gilmore, 1993; Rapoport et al., 2004; Sabatini and Adesnik, 1995; Walter and Johnson, 1994). We will refer to this functional entity as the translocon complex (TC). Overall, the inactive TC alone is comprised of more than 20 polypeptides, including the subunits of the oligosaccharyltransferase (OST) (Johnson and van Waes, 1999; Nilsson et al., 2003; Rapoport et al., 1996). The molecular mass of the TC totals approximately 950 kDa and, all together, it may contain up to 78 transmembrane domains (TMDs) (Johnson and van Waes, 1999; Nilsson et al., 2003; Rapoport et al., 1996) (see also, Calculation of the sizes of translocon assemblies, in Materials and Methods). Evidence for the size and composition of the TC comes also from recent structural studies on membrane-bound ribosomes isolated under conditions that preserve their interaction with the TC, showing an overall diameter of the TC of about 125 Å (Menetret et al., 2000). An active TC carries a ribosome (250 Å in diameter), which has a molecular mass of about 5000 kDa and may also be associated with other cytosolic factors (McCallum et al., 2000; Rapoport et al., 1996; Walter and Johnson, 1994; Wiedmann et al., 1994). For an active TC, this would result in a mass of about 7500 kDa, with an additional 500 kDa contributed by each 1 kb of mRNA. If active TCs organized into a polysome that synthesizes a protein of 20 kDa, the structure would have the molecular mass of more than 37,000 kDa and would have at least 390 TMDs. The molecular mass and number of TMDs will proportionally increase with the size of the protein encoded by the mRNA.

Such a large structure exposed to the cytosol might be subjected to considerable friction that would impede its lateral diffusion.

We have recently described M3/18 cells expressing GFP-Dad1 fusion protein, which is functionally incorporated into the OST as one of the subunits of this complex (Nikonov et al., 2002). We have demonstrated that the lateral mobility of active TCs in the plane of the ER membrane is about seven times lower than that of the highly mobile GFP-tagged lamin B receptor (LBR-GFP). These results provided the first direct evidence that the lateral mobility of TCs in the ER membranes of the living cells is severely impaired. Assuming that the restricted mobility is only caused by friction of TMDs with the lipid bilayer, the TCs would have to be organized into very large rafts. Since large contiguous rough ER domains are characteristics of highly specialized secretory cells, and are not seen in M3/18 cells, one has to assume that the calculated diffusion constant for the TCs can not reflect only interactions of the transmembrane domains of the TCs with the lipid bilayer. Therefore, their immobilization may also be due to interactions of active TCs with cytoplasmic or lumenal proteins and structures.

Several proteins potentially mediate interactions of microtubules and the ER membranes (Amarilio et al., 2005; Andrade et al., 2004). Particularly, it has been shown that CLIMP-63, a rough-ER-specific transmembrane protein (Schweizer et al., 1995), can interact with microtubules via its cytosolic domain (Klopfenstein et al., 1998) and probably MAP2 (Farah et al., 2005). Moreover, the lumenal domain of CLIMP-63 (also known as CKAP4, cytoskeleton-associated protein 4) promotes the oligomerization and almost complete immobilization of this protein in the plane of the ER membrane (Klopfenstein et al., 2001). It has also been shown that overexpression of certain CLIMP-63 mutants resulted in rearrangements and co-alignments of the ER membranes with microtubules in COS-1 cells (Vedrenne et al., 2005). Here, we present results, indicating that these cytoskeletal elements play indeed a role in restricting the lateral mobility of TCs in the ER membranes.

Results

We have previously demonstrated that the GFP-Dad1 fusion protein stably expressed in M3/18 cells is quantitatively and functionally incorporated into the OST and, therefore, it can be used as a reporter molecule for the lateral mobility of the TCs (Nikonov et al., 2002). As determined by FRAP, the lateral mobility of GFP-Dad1-tagged TCs was much more restricted than expected from its estimated size. In the experiments shown here, FRAP analysis was performed on M3/18 cells essentially as described earlier (Nikonov et al., 2002), except that all experiments were carried out using the environmental chamber (Zeiss) with a heated (39.5°C) stage set and by supplying humidified air containing 10% CO_2.

In our previous FRAP experiments done at room temperature, we reported the diffusion coefficient for LBR-GFP fusion protein to be D_{eff}=0.331 μm^2/second (Nikonov et al., 2002). As expected, the lateral mobility for LBR-GFP was slightly higher at 39.5°C (D_{eff}=0.391 μm^2/second) (Table 1). The new value of the diffusion constant for LBR-GFP fusion protein is in good agreement with results reported by others (Ellenberg et al., 1997). Under the same new experimental conditions, the lateral mobility of GFP-Dad1, representing the TCs in untreated cells, was somewhat higher (D_{eff}=0.060 μm^2/second) (Table 1) than previously reported (D_{eff}=0.049 μm^2/second) (Nikonov et al., 2002). The new data confirmed our earlier findings that the lateral mobility of the TCs is severely restricted in M3/18 cells. The treatment of cells with cycloheximide (CHX), resulting in the inhibition of protein synthesis at the stage of polypeptide elongation, had no significant effect on the lateral mobility of the GFP-Dad1 construct (D_{eff}=0.070 μm^2/second), indicating that the mobility of the TCs was not affected by this treatment (Table 1). To exclude that CHX affects the mobility of membrane proteins unspecifically, BHK-21 cells expressing LBR-GFP were treated with the same concentration of the drug. In FRAP experiments, no significant difference was detected in the lateral mobility of this GFP-tagged membrane protein expressed in control (D_{eff}=0.391 μm^2/second) and drug-treated cells (D_{eff}=0.386 μm^2/second) (Table 1). By contrast, treatment

Table 1. The lateral mobility of TCs in M3/18 cells is increased by treatments that inhibit protein synthesis or affect microtubule integrity

						Calculated TC assemblies*	
Cell line	GFP-tagged reporter	Treatment	D_{eff} (μm^2/s) ± s.d.	*n*	*P*(T⩽t)	Radius (nm)	*n* of TCs
BHK-21	LBR-GFP	–	0.391±0.120	15	–	0.5	–
		CHX	0.386±0.060	7	0.907	0.5	–
		NC	0.385±0.154	17	0.910	0.5	–
M3/18	GFP-Dad1	–	0.060±0.009	34	–	338†	5867†
		CHX	0.070±0.023	12	0.275	133†	912†
		PU	0.165±0.045	14	<0.001	5	1.5
		NaCl	0.144±0.051	12	0.008	8	3
		CHX + NaCl	0.073±0.012	8	0.056	106†	516†
		LB	0.061±0.013	10	0.950	304†	4738†
		NC	0.104±0.026	25	<0.001	21	24
		NC + PU	0.158±0.043	10	<0.001	6	2
		Taxol	0.079±0.019	8	0.017	71†	255†

NC, nocodazole; CHX, cycloheximide; PU, puromycin; LB, lantrunculin B.

*, Calculation of radii of TC assemblies are based on the diffusion constants (D_{eff}) as determined by FRAP. The equation used to calculate these radii takes into account only friction of the transmembrane domains with the lipid bilayer.

†, Radius values and number (*n*) of TCs in TC assemblies, obtained under experimental conditions where microtubules remained intact. Radius values are therefore expected to be much higher than the actual size of the TC assemblies owing to the contribution of microtubules that interfere with the free diffusion TCs. See also Materials and Methods for a more detailed explanation related to these calculations.

of the cells with puromycin, which causes termination of protein synthesis and disassembly of polysomes (Adelman et al., 1973; Vazquez, 1974), resulted in an almost threefold increase in the diffusion rate of the TCs (D_{eff}=0.165 μm^2/second). Readout of polysomes in M3/18 cells caused by adding NaCl to a final concentration of 300 mM to the growth medium (Saborio et al., 1974; Wengler, 1972) led almost to the same increase in lateral mobility of the TCs (D_{eff}=0.144 μm^2/second) as that observed in the cells treated with puromycin alone (Table 1). However, pretreatment of the cells with CHX before raising the NaCl concentration to 300 mM abolished the effect of elevated NaCl concentration on the lateral mobility of the TCs (D_{eff}=0.073 μm^2/second). This may be expected because CHX-pretreatment prevents the polysomal read-out caused by elevated NaCl concentrations.

Nocodazole treatment of M3/18 cells results in an increased lateral mobility of the TC

One of the possible explanations for the reduced lateral mobility of the TCs in M3/18 cells is that the TCs are organized into rafts that define the rough domain of the ER. In addition, the free diffusion of active TCs can be hindered through nonspecific interactions with cytoskeletal elements positioned in close proximity to the ER membrane that may have a specific role in organizing the rough domain of the ER. To test this notion, we performed FRAP experiments on M3/18 cells treated with drugs that affect the integrity of the cytoskeleton. Latrunculin B, a compound isolated from the Red Sea sponge *Latrunculia magnifica*, effectively depolymerizes microfilaments (Spector et al., 1989; Wakatsuki et al., 2001). Treatment of M3/18 cells with latrunculin B (10 μM for 2 hours) had no effect on the lateral mobility of the TCs (D_{eff}=0.061 μm^2/second), indicating that actin filaments are not involved in stabilization of the rough domain of the ER (Table 1). However, incubation of the cells with nocodazole (33 μM for 4 hours), a microtubule-depolymerizing drug, resulted in an increase of the lateral mobility of GFP-Dad1 (D_{eff}=0.104 μm^2/second), suggesting that microtubules plays a role in the immobilization of TCs. The addition of puromycin to nocodazole-pretreated cells resulted in even faster diffusion of the TCs (D_{eff}=0.158 μm^2/second), which was the same as that observed in cells treated with puromycin alone (D_{eff}=0.165 μm^2/second; Table 1). We have shown previously that puromycin treatment does not affect the lateral mobility of LBR-GFP (Nikonov et al., 2002). Here, we show that nocodazole treatment also does not affect the diffusion coefficient of this GFP-tagged membrane protein (D_{eff}=0.385 μm^2/second; Table 1). One might expect that, if microtubules, which are highly dynamic structures, play a role in the immobilization of TCs, their stabilization has no effect on the lateral diffusion of TCs or might even reduce it. Taxol has been shown to stabilize microtubules by promoting polymerization of tubulin subunits in vitro (Schiff et al., 1979) and in living cells (Yvon et al., 1999). However, we have observed a slight but statistically significant increase in the lateral mobility of TCs in taxol-treated M3/18 cells (D_{eff}=0.079 μm^2/second; Table 1). One possible explanation for this observation is that taxol treatment causes individual microtubules to form thick bundles (Jordan et al., 1993), which in turn may reduce the density of microtubules located in close proximity to the ER.

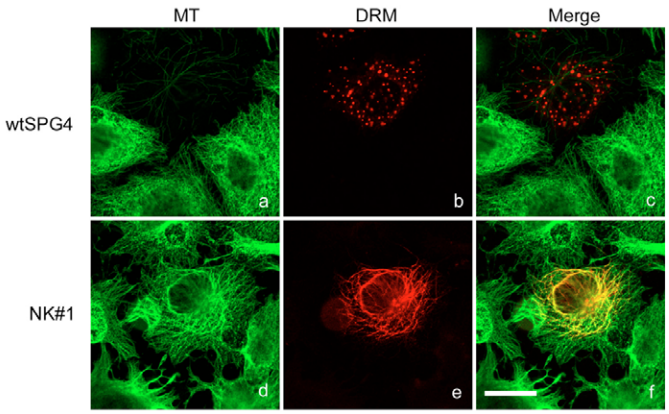

Fig. 1. DRM-tagged wild-type spastin (wtSPG4) severs microtubules in COS-1 cells. Cos-1 cells seeded on glass coverslips were transfected with plasmids encoding the fusion proteins DRM-wtSPG4 or DRM-NK#1. After fixation, cells were immunolabeled with anti-α-tubulin monoclonal antibody and secondary antibody conjugated to Alexa Fluor-633. Images were collected with a LSM510 microscope equipped with a Plan-Apochromate 100×/1.4 oil DIC lens at scan-zoom set at '1', line average set at '4' and pinhole set to optical slice of 0.5 μm. The HeNe2 laser was used to visualize microtubules (a,d) and the HeNe1 laser was used to visualize the DRM-tagged constructs (b,e). The channel representing immuno-labeled microtubules was pseudo-colored in green. Most of microtubules are severed in the cells expressing DRM-wtSPG4 (a-c). The DRM-wtSPG4 fusion protein has a characteristic punctate distribution. Expression of the biologically inactive DRM-NK#1 construct leads to the decoration of intact microtubules by the fusion protein (d-f). Bar, 20 μm.

Expression of the microtubule-severing ATPase spastin in M3/18 cells accelerates the lateral mobility of the TCs

The increased lateral mobility of GFP-Dad1 observed in M3/18 cells treated with nocodazole suggested that the state of assembly of microtubules affects the lateral mobility of the TCs. Although no inhibitory effect of nocodazole on protein synthesis had been observed (Rennison et al., 1992), one may argue that unspecific side effects of this drug could have caused the observed results. Therefore, we expressed the microtubule-severing protein spastin, also know as SPG4 (Ogura and Wilkinson, 2001), in M3/18 cells and studied its effects on the mobility of the TCs. According to recent studies, wild-type SPG4 (wtSPG4) binds specifically to microtubules and effectively breaks them down, whereas an inactive mutant (NK#1) binds microtubules but leaves them intact (Evans et al., 2005). In order to identify transfected M3/18 cells to be analyzed by FRAP experiments, we expressed fusion proteins where the C-terminus of the monomeric red fluorescent protein (DRM) precedes the N-termini of wtSPG4 or NK#1. The fusion proteins were named DRM-wtSPG4 and DRM-NK#1, respectively. The cellular localization of these fusion proteins and their effect on the microtubules were visualized by immuno-fluorescent microscopy in COS-1 cells. These cells, in contrast to M3/18 cells, are rather flat and allow patterns of microtubules to be more easily demonstrated. DRM-wtSPG4 expressed in COS-1 cells has a characteristic punctate cellular localization (Fig. 1b). Moreover, the expression of DRM-wtSPG4 in COS-1 cells led to an almost complete breakdown

Table 2. Increased lateral mobility of GFP-tagged TCs in M3/18 cells expressing DRM-tagged spastin or a CLIMP-63 deletion mutant lacking the microtubule-binding domain

Cell line	GFP-tagged reporter	DRM-tagged construct	D_{eff} (μm^2/s) ± s.d.	*n*	*P*(T≤t)	Calculated TC assemblies*	
						Radius (nm)	*n* of TCs
BHK-21	LBR-GFP	–	0.391±0.120	15	–	0.5	–
		p63-DRM	0.391±0.045	6	0.999	0.5	–
M3/18	GFP-Dad1	–	0.060±0.009	34	–	338	5867
		DRM-wtSPG4	0.125±0.024	7	<0.001	11	7
		DRM-NK#1	0.058±0.011	9	0.612	423	9196
		p63-DRM	0.063±0.007	7	0.672	248	3154
		ΔLp63-DRM	0.059±0.012	18	0.643	350	8763
		DRM-ΔCp63	0.088±0.021	14	0.001	93	93
		ΔTLp63-DRM	0.098±0.013	5	0.001	37	37
		DRM	0.053±0.010	7	0.182	–	–

*Since microtubules remain intact in all experiments, except in the one where FRAP was done on the cells expressing spastin (DRW-wtSPG4), the calculated radius values and the numbers (*n*) of TC assemblies are overestimated because of interactions of the TCs with microtubules. See also footnote to Table 1 and see Materials and Methods on the calculation of the sizes of TC assemblies.

of microtubules (Fig. 1a-c), while DRM-NK#1 expressed in the same cell line, primarily decorated microtubules (Fig. 1e) without causing their breakdown (Fig. 1d-f). Our data on the localization and the effect of these two fusion proteins on microtubules are similar to those reported for the GFP-tagged wtSPG4 and NK#1 fusion proteins (Evans et al., 2005), confirming that substitution of the GFP tag for DRM did not affect the biological properties of the proteins.

In order to determine the effect of spastin on the lateral mobility of the TCs, M3/18 cells were transfected with the recombinant plasmids encoding the DRM-wtSPG4 or DRM-NK#1 constructs. The following day, lateral mobility of the stably expressed GFP-Dad1 was measured in transfected cells. It was found that expression of the DRM-wtSPG4 fusion protein was accompanied not only by microtubule breakdown (Fig. 1a), but also by an increase in the lateral mobility of the TCs (D_{eff}=0.125 μm^2/second; Table 1). However, the lateral mobility of the TCs remained unchanged at D_{eff}=0.058 μm^2/second (Table 2) in cells expressing the DRM-NK#1 construct, which does not affect the state of microtubules (Fig. 1d-f).

Effects of the expression of CLIMP-63 related fusion proteins on the lateral mobility of the TCs in M3/18 cells

It has been shown previously that some microtubules are located in close proximity to the ER membranes (Marsh et al., 2001). Furthermore, these cytoskeletal elements interact with the cytosolic domain of CLIMP-63, a type II transmembrane protein that resides in the ER (Klopfenstein et al., 1998). Moreover, the lumenal domain of CLIMP-63 has the ability to form oligomers and the wild-type protein is practically immobilized by forming a network in the plane of the ER membrane. The diffusion coefficient for this GFP-tagged protein was calculated to be even lower (D_{eff}=0.015 μm^2/second) (Klopfenstein et al., 2001) than that for the TCs. Therefore, it was of interest to see whether overexpression of the wild-type CLIMP-63 and of several deletion mutants have an effect on the lateral mobility of TCs in M3/18 cells. The expression and functionality of GFP-tagged wild-type CLIMP-63 and its deletion mutants have been characterized previously (Klopfenstein et al., 2001). An important finding of this work was that the GFP tag does not interfere with the biological functions of CLIMP-63. To identify in M3/18 cells the transiently expressed CLIMP-63-related constructs we replaced the GFP tag in the previously described CLIMP-63 fusion proteins with the DRM tag to distinguish it optically from GFP-Dad1. In all, we made four DRM-tagged CLIMP-63 related deletion constructs: p63-DRM, ΔLp63-DRM, DRM-ΔCp63 and ΔTLp63-DRM. Schematic representations of these constructs are shown in Fig. 2A. M3/18 cells were transiently transfected with these constructs, and western blot analysis demonstrated that each of the constructs can be expressed in M3/18 cells and the expressed fusion proteins had the predicted electrophoretic mobility (Fig. 2B).

The intracellular localization of these DRM-tagged constructs expressed in M3/18 cells was visualized by fluorescent microscopy (Fig. 3). In the p63-DRM fusion protein, the C-terminus of the wild-type human CLIMP-63 was fused with the N-terminus of DRM (Fig. 2A). Like the GFP-tagged CLIMP-63 expressed in COS-1 cells (Klopfenstein et al., 2001), the DRM-tagged construct expressed in M3/18 cells has the typical ER localization, with a fine reticular network permeating the entire cytoplasmic compartment (Fig. 3b). Moreover, GFP-Dad1 stably expressed in M3/18 cells (Fig. 3a) colocalized with p63-DRM (Fig. 3c). The ΔLp63-DRM fusion protein, where the luminal domain of CLIMP63 was replaced by the DRM tag (Fig. 2A), can still bind to microtubules. However, it can no longer form oligomers in the plain of the ER membranes (Klopfenstein et al., 2001). As may be expected from results obtained with the GFP-tagged deletion construct (Klopfenstein et al., 2001), ΔLp63-DRM expressed in M3/18 cells also colocalized with GFP-Dad1 (Fig. 3d-f). In the DRM-ΔCp63 construct, the cytosolic microtubule-binding N-terminal domain of CLIMP63 was substituted by the DRM tag (Fig. 2A). Therefore, this fusion protein lacks the ability to bind microtubules while retaining the ability to form the oligomers (Klopfenstein et al., 2001). It also co-localizes with GFP-Dad1 (Fig. 3i), and it appears that at least a part of the overexpressed DRM-ΔCp63 is integrated throughout the ER into the spatial network formed by endogenous CLIMP-63, thus reducing overall the density of microtubule-binding sites. However, a significant amount of this fusion protein was concentrated in the perinuclear region (Fig. 3h), which was not the case for GFP-Dad1 (Fig. 3g). As expected, a soluble fusion protein ΔTLp63-DRM, in which the DRM tag was fused to the cytosolic microtubule-binding domain of CLIMP-63 (Fig. 2A), had a cytosolic and nuclear localization, and did not colocalize with GFP-Dad1 (Fig. 3j-l). A similar

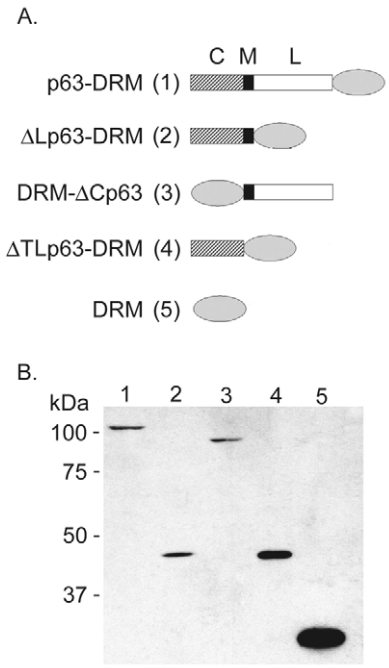

Fig. 2. DRM-tagged CLIMP-63 related constructs expressed in M3/18 cells have the molecular mass expected. (A) Schematic representation of CLIMP-63 related constructs tagged with the red fluorescent protein (DRM) of *Discosoma sp*. CLIMP-63 is a type II transmembrane protein. It has a relatively short N-terminal cytosolic domain (hatched box), which is capable of binding to microtubules. A larger C-terminal lumenal domain (open box) can form oligomers. The transmembrane domain is represented by a black box. Monomeric DRM used as a tag is represented as a gray oval. (B) The cells transfected with recombinant plasmids encoding p63-DRM (lane 1), ΔLp63-DRM (lane 2), DRM-ΔCp63 (lane 3), ΔTLp63-DRM (lane 4) or the cloning vector encoding DRM (lane 5) were subjected to western blot analysis using a commercial M3/18 directed against the red fluorescent protein. All expressed fusion proteins had the expected molecular mass.

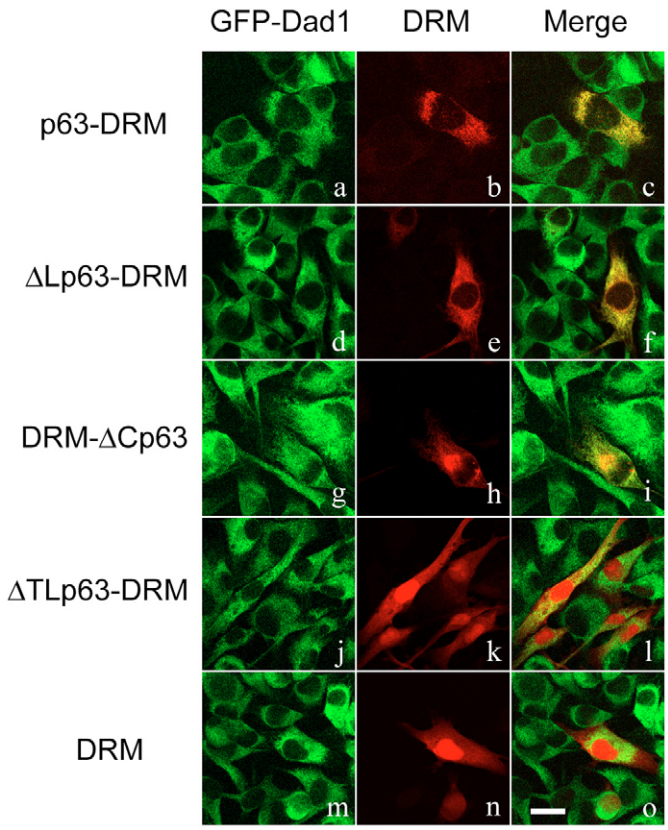

Fig. 3. Intracellular localization of DRM-tagged CLIMP-63 related constructs in M3/18 cells. M3/18 cells grown at 39.5°C were transfected with recombinant plasmids encoding the corresponding fusion proteins. Images were collected with an LSM510 microscope equipped with a Plan-Apochromate 100×/1.4 oil DIC lens at scan-zoom set at '1' and line average set at '4'. Due to low fluorescent intensity of stably expressed GFP-Dad1 the pinholes were set wide-open. Expression of GFP-Dad1 was visualized using the argon laser (a,d,g,j,m). The HeNe1 laser was used to visualize DRM-tagged constructs (b,e,h,k,n). To assess colocalization of two proteins, the images of both channels were merged (c,f,i,l,o). Expression of p63-DRM and ΔLp63-DRM fusion constructs revealed that these fusion proteins are localizing to the ER (a-c and d-f, respectively). No changes in the ER morphology were observed. Expression of the soluble ΔTLp63-DRM and DRM revealed that these proteins are localizing to the cytosol (j-l and m-o, respectively). The morphology of the ER is not altered. Expression of the DRM-ΔCp63 construct lead to some accumulation in a perinuclear area, while the morphology of the ER appeared was not affected (g-i). ΔTLp63-DRM apparently had cytosolic localization (j-l) similar to that of red fluorescent tag, DRM (m-o). Bar, 20 μm.

localization pattern was observed for the soluble DRM, expressed in M3/18 cells (Fig. 3m-o).

The lateral mobility of the GFP-Dad1-tagged TCs was determined in M3/18 cells expressing the DRM-tagged CLIMP-63-derived constructs using the FRAP technique. The expression of p63-DRM in M3/18 cells did not affect the lateral mobility of the TCs (D_{eff}=0.063 μm^2/second in transfected cells versus D_{eff}=0.060 μm^2/second in control cells; Table 2). Also, transfection of M3/18 cells with the plasmids encoding ΔLp63-DRM or DRM had no effect on the lateral mobility of the TCs. The D_{eff} values for the TCs in the cells expressing these constructs were 0.059 μm^2/second or 0.053 μm^2/second, respectively (Table 2). However, expression of the DRM-ΔCp63 fusion protein resulted in a statistically significant increase of the lateral mobility of the TCs from D_{eff}=0.060 μm^2/second in control cells to 0.088 μm^2/second in cells expressing the deletion construct (P=0.001, Table 2). Expression of the soluble fusion protein containing only the microtubule binding domain, ΔTLp63-DRM, resulted in an even greater increase of the diffusion coefficient of the TCs (D_{eff}=0.098 μm^2/second; Table 2). It is interesting that the level of ΔTLp63-DRM expression was much higher than that of DRM-ΔCp63 as judged from the western blotting results (Fig. 2B). The high level of expression and the solubility of ΔTLp63-DRM may have resulted in the preferential binding of microtubules to this constructs rather than to the endogenous CLIMP-63, thus reducing the density of the microtubules attached to the ER. In order to assess the possible effects of overexpressed membrane proteins, such as CLIMP-63, on the lateral mobility of LBR-GFP, we co-expressed p63-DRM and LBR-GFP in BHK-21 cells. We did not observe changes in the lateral mobility of LBR-GFP

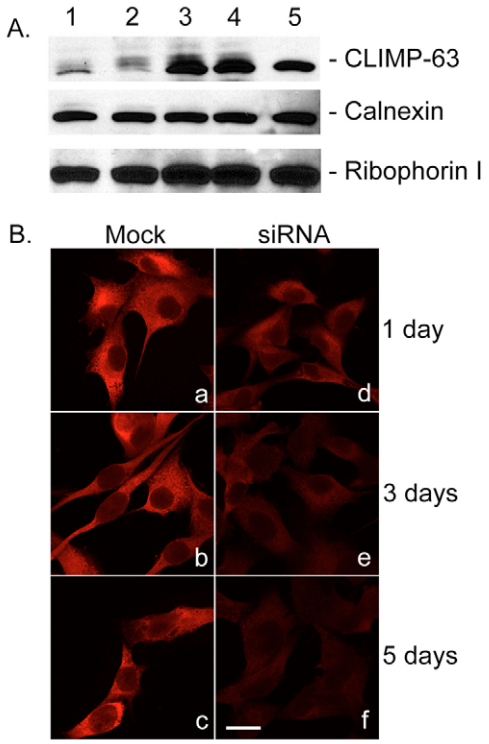

C.

Construct	Nucleofection	D_{eff}, (μm^2/sec) ± s.d.	n
GFP-Dad1	-	0,063 ± 0,012	11
	Mock	0,067 ± 0,011	10
	siRNA	0,137 ± 0,029	21
LBR-GFP	-	0,391 ± 0,120	15
	siRNA	0,385 ± 0,055	7

(D_{eff}=0.391 μm^2/second) compared with those in control cells (Table 2).

Knock-down of CLIMP-63 by siRNA increases the lateral mobility of the TCs in M3/18 cells

Overexpression of the DRM-ΔCp63 construct, which lacks the microtubule binding domain, resulted in some increase of the lateral mobility of the TCs in M3/18 cells. This limited effect may be due to the fact that overexpression of this construct did not eliminate completely the microtubule-binding sites in the ER. Instead, the microtubule binding sites were merely 'diluted' by the interspersed CLIMP-63 construct lacking the microtubule binding domain. If this argument were correct, a knock-down of the endogenous CLIMP-63 expression would lead to an even higher lateral mobility of the TCs. Therefore, we used RNA interference (RNAi) to silence expression of CLIMP-63 in M3/18 cells. Three small interfering RNAs (siRNAs) were designed. The first two, siRNA#1 and siRNA#2, were manually selected from conserved regions of the CLIMP-63 nucleotide sequence using the BLOCK-iT™ RNAi Designer Computer Program (Invitrogen). The third one (siRNA#3), a SIGenome Smart pool reagent, was designed by Dharmacon. M3/18 cells were transfected with siRNA using the Amaxa nucleofection system. Cells were collected 4 days after nucleofection and samples were subjected to western blot analysis. Transfection of M3/18 cells with siRNA#1 and siRNA#2 resulted in essentially complete knock-down of CLIMP-63 (Fig. 4A, lanes 1 and 2). However, transfection with siRNA#3 did not seem to have an effect on CLIMP-63 expression (Fig. 4A, lane 3), because expression levels remained similar to those of mock-transfected and untreated cells (Fig. 4A, lanes 4 and 5, respectively). Knock-down of CLIMP-63 using siRNA#1 and siRNA#2 seemed specific because it had no effect on the expression of two other ER proteins calnexin and ribophorin I (Fig. 4A).

The effectiveness of CLIMP-63 knock-down was also assessed by immunofluorescence microscopy. M3/18 cells mock-transfected (Fig. 4Ba-c) or transfected with siRNA#2 (Fig. 4Bd-f) were fixed and stained with an anti-CLIMP-63 rabbit polyclonal antibody (pAb) on day one, 3 or 5 days after transfection. After 1 day, immunostaining of the mock-transfected cells revealed a typical ER pattern (Fig. 4Ba). The intensity of the staining was similar to that of untreated cells (data are not shown), and the CLIMP-63 staining patterns or the intensity of the ER staining did not change in cells 3 or 5 days after transfection (Fig. 4b or c, respectively). At 1 day after transfection with siRNA#2, ER localization of CLIMP-63 was still seen, although, the staining intensity was substantially lower than in control cells (Fig. 4Bd).

Fig. 4. siRNA knock-down of CLIMP-63 expression led to an increased lateral mobility of the TCs in M3/18 cells. (A) Western blot analysis of M3/18 cells transfected with siRNA#1 (lane 1), siRNA#2 (lane 2), siRNA#3 (lane 3), mock transfected (lane 4) or untreated (lane 5). The samples were collected 4 days after transfection. Staining of the western blot with anti-CLIMP-63 pAb shows that siRNA#1 and siRNA#2 are able to silence the expression of CLIMP-63 in M3/18 cells (lanes 1 and 2), wheras siRNA#3 had no effect on CLIMP-63 expression (lane 3) when compared with mock-transfected (lane 4) or untreated (lane 5) cells. The staining of the same blot with anti-calnexin or anti-ribophorin I pAbs revealed that expression levels of these proteins were not affected by the CLIMP-63 knock-down. (B) Immuno-fluorescent microscopy of mock-transfected cells (a-c) or cells transfected with siRNA#2 (d-f). The cells were collected on day 1,3 and 5 after transfection, fixed in 2% PFA in PBS and stained with anti-CLIMP-63 pAb followed by goat anti-rabbit IgG conjugated to Alexa Fluor-543. The images were collected with the LSM510 microscope equipped with a HeNe1 laser and a Plan-Apochromate 100×/1.4 oil DIC lens at scan-zoom set at '1' and line average set at '4'. The pinhole was set to obtain 0.5 μm thick optical slices. The immunofluorescence microscopy results support western blot data showing that siRNA#2 can effectively knock down of CLIMP-63 expression.Bar, 20 μm. (C) FRAP analysis of untreated M3/18 cells confirmed our previous findings that the lateral mobility of the TCs is very low (D_{eff}=0.063 μm^2/second). FRAP analysis of mock-transfected cells performed at the day 4 after transfection suggested that electro-shocking of the cells suspended in transfection buffer had no effect on the TC mobility (D_{eff}=0.067 μm^2/second, $P(T \leq t)$=0.427). However, transfection of the cells with siRNA#2 led to an increased diffusion rate of the TCs (D_{eff}=0.137 μm^2/second, $P(T \leq t)$<0.001). Knock-down of CLIMP-63 with siRNA had no effect on the lateral mobility of the ER membrane protein LBR-GFP.

At 3 days after nucleofection with siRNA#2, immunostaining intensity was greatly reduced (Fig. 4Be) and ER staining was even further reduced on day 5 (Fig. 4Bf).

Taken together, the results obtained by western blot analysis and fluorescence microscopy suggested that siRNA#1 and siRNA#2 are able to greatly reduce the expression of CLIMP-63 in M3/18 cells. Cells were transfected with siRNA#2 and used on day 4 after transfection for FRAP experiments. FRAP analysis of untreated M3/18 cells, performed independently of the experiments presented in Tables 1 and 2, confirmed earlier findings that the TCs are diffusing slowly (D_{eff}=0.063 μm^2/second) (Fig. 4C). The lateral mobility of the TCs in mock-transfected cells was similar to that in untreated cells (D_{eff}=0.067 μm^2/second), suggesting that nucleofection itself does not affect the lateral mobility of the TCs (Fig. 4C). However, the knock-down of CLIMP-63 expression in M3/18 cells led to a significant increase in the lateral mobility of the TCs, with D_{eff} values increasing from 0.067 μm^2/second in mock-transfected cells to 0.137 μm^2/second in the cells transfected with siRNA#2 (Fig. 4C). One may argue that the knock-down of CLIMP-63 in itself could increase the lateral mobility of the ER proteins because the the ER membrane is less crowded by membrane proteins. Therefore, 2 days after nucleofection of BHK-21 cells with anti-CLIMP-63 siRNA, cells were transfected with the plasmid DNA encoding LBR-GFP. After 1 or 2 days, cells expressing LBR-GFP were subjected to FRAP analysis. The calculated D_{eff} value for LBR-GFP in these cells remained similar to that in control cells (Fig. 4).

Discussion

Ultrastructural studies on certain secretory cells have demonstrated a sharp transition between the rough and smooth ER, which are part of a continuous membrane system but represent morphologically and functionally distinct domains (Borgese et al., 2006; Fawcett, 1966; Shibata et al., 2006; Voeltz et al., 2002). It has also been shown that membrane-bound polysomes are arranged in regular figures (Christensen and Bourne, 1999; Christensen et al., 1987). Moreover, when rough microsomes were solubilized with non-ionic detergents, curved membrane remnants were obtained, in which ribosomes were attached to a proteinaceous fibrillar meshwork that was insensitive to RNase treatment (Kreibich et al., 1978; Marcantonio et al., 1982). All these experimental data suggested that TCs are not able to defuse freely in the plane of the ER membrane. Our recent FRAP experiments on M3/18 cells demonstrated that the diffusion rate of the TCs is indeed very low (Nikonov et al., 2002). However, ribosome-size dextran particles are highly mobile in protein solutions with concentrations similar to those found in the cytoplasm (Bierer et al., 1987; Lippincott-Schwartz et al., 2001; Zhang et al., 1991), suggesting that the friction of membrane-bound ribosomes with soluble cytoplasmic proteins does not significantly contribute to the TC immobilization. These findings prompted us to hypothesize that TCs are organized into large rafts by direct or indirect interactions among the TCs and/or with other components of the ER or cytoplasm. The organization of the TCs into raft-like assemblies might provide a more efficient environment for protein synthesis on membrane-bound polysomes (Sabatini and Kreibich, 1976). This notion is supported by experiments, showing that the induction of amylase synthesis in AR42J cells by dexamethasone treatment resulted in a striking rearrangement of the rough ER from a tubulo-vesicular configuration into stacks of cisternae without an increase in the number of membrane-bound ribosomes (Rajasekaran et al., 1993).

The results obtained by the FRAP experiments described here confirm our previous findings that the lateral mobility of the TCs is severely restricted (Table 1). Here, we have shown that depolymerization of microtubules by nocodazole treatment of the cells increased the diffusion rate of the TCs (Table 1). Our interpretation of the drastic changes in the diffusion coefficient caused by the depolymerization of microtubules is that the slow diffusion of TCs in untreated control cells is mainly due to the restrictions imposed on the lateral mobility of these large oligomeric structures by intact microtubules. Overexpression of spastin, a microtubule-severing protein, also increased the lateral mobility of TC assemblies, resulting in a calculated size that corresponds to about 27 TCs. This aggregation size might still be artificially high due to interactions of TCs with some remaining, not completely depolymerized microtubules (Table 2 and Fig. 1a). It appears, therefore, that depolymerization of microtubules affects the lateral mobility of TCs by dissolving the diffusion barriers membrane-bound polysomes. This notion is supported by the findings that the elaborate network of tubules and cisternae of the ER is stabilized by microtubules (Dabora and Sheetz, 1988; Storrie et al., 1998; Dreier and Rapoport, 2000). Furthermore, the ultrastructural reconstructions of the 3D arrangement of cellular organelles showed that microtubules are, in fact, in very close proximity to ER membranes (Marsh et al., 2001). Our finding that treatment of M3/18 cells with the microtubule-stabilizing drug taxol resulted in a significant increase of the diffusion rate of the TCs (Table 1) seems to be somewhat paradoxical. A possible explanation is provided by the observation that treatment of HeLa cells with taxol resulted not only in an increase of microtubule mass (Jordan et al., 1993), but microtubules also undergo major rearrangements by forming the bundles (Jordan et al., 1993; Yvon et al., 1999) resulting in microtubule-free zones (Schiff and Horwitz, 1980). It should be noted, however, that the calculated size of the TC assemblies in taxol-treated cells was still significantly larger than those in cells treated with nocodazole or expressing the DRM-wtSPG4 construct (Tables 1 and 2). Our data also show that, unlike microtubules, the state of actin filament assembly had no effect on the immobilization of the TCs, because the diffusion coefficient and the calculated size of the TC rafts remained unchanged, when M3/18 cells were treated with latrunculin B (Table 1).

The rough-ER-specific membrane protein CLIMP-63 tethers microtubules to the ER (Farah et al., 2005; Vedrenne et al., 2005) and might, therefore, play a major role in mechanisms that affect the lateral mobility of membrane-bound polysomes. Homotypic interactions among the large lumenal domains of CLIMP-63 promote its oligomerization and thus the formation of a network at the luminal face of ER membranes, FRAP analysis has shown that this membrane protein is practically immobilized (D_{eff}=0.015 μm^2/second) (Klopfenstein et al., 2001). The cytoplasmic domain of this type II transmembrane protein carries a microtubule-binding domain (Klopfenstein et al., 1998). Overexpression of CLIMP-63 had no effect on the lateral mobility of TCs in

M3/18 cells, indicating that new microtubule-binding sites might not promote additional binding of microtubules to the ER. A possible explanation is that the amount of MAP2-like proteins, which may mediate the binding of microtubules to CLIMP-63 (Farah et al., 2005; Vedrenne et al., 2005), is limited, thus leaving some ER-microtubule-binding sites empty. However, expression of the DRM-ΔCp63 fusion protein resulted in a significant increase in the lateral mobility of the TC (from D_{eff}=0.060 μm^2/second to D_{eff}=0.088 μm^2/second), which corresponds to a reduction of the apparent size of the TC assemblies (Table 2). This increase in the diffusion rate of the TCs was less pronounced than that seen after treatment of the cells with nocodazole. This might be because endogenous CLIMP-63 is a very stable protein (with a half life of about 24 hours) and was still expressed in these cells. Therefore, the density of endogenous CLIMP-63 in the ER membrane might only be reduced by the overexpressed DRM-ΔCp63 construct and, unlike in nocodazole-treated cells, some microtubules are expected to be still attached to the ER in DRM-ΔCp63-transfected cells. Knock-down of CLIMP-63 expression by using siRNA and elimination of the ER-microtubule-binding sites provided by this protein, resulted in a substantial increase of the lateral mobility of the TCs from D_{eff}=0.067 μm^2/second to D_{eff}=0.137 μm^2/second (Fig. 4C). The apparent size of the TC assemblies in cells transfected with siRNA#2 was reduced to the size of a small polysome (Fig. 4). These findings further support the notion that microtubules might play a role in restraining the lateral mobility of active TCs.

An important finding was that an increase in lateral mobility of the TCs is less pronounced in cells treated with nocodazole (D_{eff} increased from 0.060 μm^2/second to 0.104 μm^2/second), or cells expressing the microtubule-severing DRM-wtSPG4 construct (D_{eff} increased to 0.102 μm^2/second), compared with cells treated with puromycin (D_{eff}=0.165 μm^2/second), or with elevated concentrations of NaCl (D_{eff}=0.144 μm^2/second; Tables 1 and 2). Breakdown of microtubules reduced the calculated size of TC assemblies, which in untreated cells appeared as artificially large surface areas, to the size of large polysomes in nocodazole-treated cells (Table 1). We would like to stress that the large size of TC assemblies obtained in our calculations for untreated cells is mainly owing to the fact that the equation used takes into account only friction of the transmenbrane domains of the TCs with the lipid bilayer. The impediment in the free lateral mobility due to interactions of microtubules with TCs results in the artificially large calculated sizes of the TC assemblies. In NaCl- or puromycin-treated cells, which have an intact network of microtubules, calculated sizes of the TC assemblies were reduced to the size of individual TC (Table 1). A small, single-membrane-spanning protein, such as LBR-GFP is not affected by the nocodazole-mediated disassembly of microtubules, indicating that the drug treatment itself does not affect the diffusion properties of membrane proteins. It appears, therefore, that large assemblies, such as polysomes, were restraint in their mobility by intact microtubules, whereas small membrane proteins or even large multi-subunit complexes, such as single TCs, essentially diffused according to their calculated diffusion coefficient, when only friction of transmembrane domains with the lipid bilayer is considered. It is interesting to note that treatment of M3/18 cells with puromycin or NaCl resulted in a reduction of the translocon assemblies to the size of an individual TC. An interpretation of these results should take into consideration recent results, which indicate that after puromycin treatment of cells, inactive ribosomes remain largely associated with the translocon (Potter and Nicchitta, 2000a; Potter and Nicchitta, 2000b; Seiser and Nicchitta, 2000). If the ribosomes remain attached to the TCs after termination of protein synthesis, they may cause additional friction. Therefore, the D_{eff} value measured under these circumstances would reflect the friction of the TC with the lipid bilayer and the ribosome with cytosolic proteins. Our electron microscopy observations suggested that the ribosomes indeed remain attached to the ER membrane in puromycin-treated AR42J cells (A.V.N. and G.K., unpublished).

A large body of evidence supports the notion that microtubules play a role in stabilizing the structure of the ER by interacting with specific sites such as CLIMP-63 (Dabora and Sheetz, 1988; Storrie et al., 1998; Terasaki et al., 1986). Recent high-resolution (6 nm) tomographical studies on a pancreatic beta cell line have mapped in great detail the spatial relationship of microtubules with respect to membrane-bound organelles (Marsh et al., 2001). It was found that, especially for the ER, the proximity to microtubules was not random, and it appeared that they had distinct association sites with this membrane system. At these sites the distances were less than 30 nm, whereas in other areas they were considerably larger. In such a model of ER-microtubule interaction one can easily envisage that small membrane proteins and even individual TCs can diffuse rather unhindered, whereas ribosomes interconnected by mRNAs that forming polysomes may become entangled at the microtubule-ER attachment sites, thus reducing substantially their free diffusion in the ER membrane. The restraint in the free lateral movement of polysomes in the plane of the ER membrane may, in fact, allow to generate differentiated rough ER domains that specialize in the synthesis of certain classes of proteins.

Materials and Methods

Antibodies and reagents

COS-1 cells were kindly provided by M. Rindler (New York University Medical Center, New York). Isolation and characterization of M3/18 cells has been reported previously (Nikonov et al., 2002). All cell cultures were grown in Dulbecco's modified Eagle's medium (DMEM) purchased from Sigma (St Louis, MO), supplemented with 10% of fetal bovine serum and L-glutamine. The anti-α-tubulin clone DM 1A monoclonal antibody (mAb; catalog number T-9026) was purchased from Sigma. Production of rabbit polyclonal antibody (pAb) directed against human CLIMP-63 was previously described (Vedrenne et al., 2005). Unless otherwise stated, endonucleases, the rapid ligation kit and other supplies for molecular biology were purchased from Roche, Indianapolis, IN. Pre-stained Precision Plus Protein Standards (Bio-Rad, Hercules, CA) were used as protein molecular mass markers. Wizard PCRPreps DNA purification system was purchased from Promega (Madison, WI). pDsRed-Monomer-N1 and pDsRed-Monomer-C1 cloning vectors, encoding a monomeric mutant derived from the tetrameric red fluorescent protein of Discosoma sp., and pAb directed against this protein were purchased from BD Biosciences, Palo Alto, CA. The plasmid construct encoding LBR-GFP was a gift from J. Lippincott-Schwartz (NIH, Bethesda, MD) and has been described before (Ellenberg et al., 1997).

Gel electrophoresis and immunoblotting

SDS-PAGE on 10-20% gradient gels and western blot analysis were performed as previously described (Nikonov et al., 1992). The BM chemiluminescence western blotting kit (Roche, Indianapolis, IN) was used to develop the blots according to the manufacturer's protocol.

Construction and expression of spastin-related (wtSPG4 and NK#1) DRM-tagged fusion proteins

The cloning of the cDNAs encoding wild-type human spastin, wtSPG4, and its biologically inactive mutant, NK#1, were previously described (Evans et al., 2005). To make the constructs, the 5′-TTTGGTACCATGAATTCTCCGGGTGGACGA-3′ and 5′-AAAGGATCCTTAAACAGTGGTATCTCCAAA-3′ primers were used to amplify both cDNAs. PCR products were purified and digested by *Kpn*I and *Bam*HI

endonucleases. Digested and purified PCR products were cloned into pDsRed-Monomer-C1. The recombinant plasmids were named pDRM-wtSPG4 and pDRM-NK#1, respectively.

Construction and expression of CLIMP-63 related DRM-tagged fusion proteins

The cloning of cDNA for human CLIMP-63 was previously described (Schweizer et al., 1993a; Schweizer et al., 1993b; Schweizer et al., 1993c). To make the constructs, the following primers were made: P63U 5′-TTTGGTACCATGC-CCTCGGCCAAACAAAG-3′, P63L 5′-AAAGGGCCCGGACCTTTTCGTGAA-TCTTCT-3′, ΔLP63L 5′-AAAGGGCCCGGTGGTGGACGCACCAGCCCG-3′, P63LS 5′-AAAGGGCCCTTAGACCTTTTCGTGAATCTTCT-3′, ΔCP63U 5′-TT-TGGTACCGGCAGGGCGCTCAACTTTCTCTT-3′, ΔTLp63L 5′-TTTGGGCC-CGCCTGCCGAGCCTGCGCGAGCAGG-3′. To generate the p63-DRM construct, P63U and P63L primers were used for PCR amplification of the cDNA encoding CLIMP-63. To construct ΔLp63-DRM, the cDNA was amplified using the P63U and ΔLP63L primers. The P63U and ΔTLp63L primers were used for PCR amplification of CLIMP-63 cDNA to make the ΔTLp63-DRM construct. The purified PCR products were subcloned into the pDsRed-Monomer-N1 cloning vector using the Kpn I and Apa I cloning sites. The DRM-ΔCp63 construct was made by PCR amplification of CLIMP-63 cDNA using the ΔCP63U and P63LS primers. The PCR product was subcloned into the pDsRed-Monomer-C1 cloning vectors using the *Kpn*I and *Apa*I cloning sites. The GC-RICH PCR System (Roche, Indianapolis, IN) was used for all PCR amplifications.

Design of anti-CLIMP-63 siRNA

The BHK-21 cell line, originally obtained from Syrian golden hamster (*mesocricetus auratus*) kidney cells, is the parental cell line for M3/18 cells (Nikonov et al., 2002). Since there are no nucleotide-sequence data available for hamster CLIMP-63, we have used two approaches in designing the siRNAs. First, we used the BLOCK-iT™ RNAi Designer program available from Invitrogen.com to select RNAi targets from the rat (*rattus norvegicus*) CLIMP-63 sequence (GenBank accession number XM_343189). To find the highly conserved ones, the resulting RNAi target sequences were blasted against mouse and human CLIMP-63 sequences (GenBank accession numbers NM_175451.1 and NM_006825.2, respectively). The following siRNAs were designed and synthesized using the services of Invitrogen: siRNA#1 5′-GCAGAAUGAGAUUCUCAAATT-3′ and siRNA#2 5′-CCAAGUCCAUCAAUGACAATT-3′, which correspond to the nucleotide positions of the rat sequences 558-579 and 671-692, respectively. In a second approach, we ordered SiGenome Smart pool reagent from Dharmacon (catalog number M-100698-00), which was designed by the company using the rat CLIMP-63 sequence. This reagent was named siRNA#3.

Transfection of mammalian cells

The Fugene 6 reagent (Gibco BRL, Grand Island, NY) was used to transfect cells according to manufacturer's protocol: 6 μl of Fugene6 reagent was added to 94 μl DMEM containing 1-2 μg of plasmid DNA. The sample was incubated at room temperature for 15 minutes and then added to the cells grown in 35-mm tissue culture dishes containing 2 ml of complete growth medium. Cells were grown overnight at 37°C in 10% CO_2.

Nucleofection of M3/18 cells and BHK-21 cells

To transfect M3/18 cells with siRNA duplexes, we used the Nucleofector II device (Amaxa Biosystems, Gaithersburg, MD) and its cell line Nucleofector Kit L (catalog number VCA-1005). The nucleofection conditions used were those established for BHK-21 cell line. After trypsinization, the cells were centrifuged at 200 ***g*** for 10 minutes. After aspiration of the medium, cells were resuspended in nucleofection solution L (10^6 cells per 100 μl of the solution). One-hundred μl of the cell suspension were added to 4 μl of siRNA stock solution and immediately transferred to the cuvette. In mock-transfection, the addition of siRNA was omitted. The cells were electroporated in the Nucleofector II device using the A-031 program. The electroporated cells were mixed with 1 ml of the complete growth medium and plated onto ordinary or glass-bottom No. 0 35-mm tissue culture dishes (MatTek, Ashland, MA). Cells were allowed to grow for 4 days before subjecting them to FRAP analysis or collecting them for western blot analysis.

Nucleofection of BHK-21 cells with siRNA duplexes was done as described for M3/18 cells. On day 3 after nucleofection, cells were transfected with plasmid DNA encoding LBR-GFP construct. The day after transfection, cells were used in FRAP experiments.

Immunofluorescence and fluorescence microscopy

The laser scanning microscope LSM510 and LSM software 3.1 (Carl Zeiss, Jena, Germany) were both used for immunofluorescence microscopy and FRAP experiments. For immunolabeling COS-1 cells grown on glass coverslips were rinsed in PBS and fixed in 2% of paraformaldehyde (PFA) in PBS for 20 minutes. PFA-fixed cells were incubated in 0.2% Triton X-100 in PBS for 2 minutes. Then, the cells were blocked in 5% skim milk in PBS for 30 minutes and incubated with mouse monoclonal anti-α-tubulin antibody (clone DM 1A, Sigma) diluted in PBS-buffered milk (1:500) at room temperature for 1 hour. After washing three times in PBS, cells were incubated for 1 hour with rabbit anti-mouse IgG Alexa Fluor-633-conjugated secondary antibody (Molecular Probes) diluted 1:500 in PBS-buffered milk, followed by three washing steps in PBS. Coverslips were mounted using Citifour Mountant Media #0 (Ted Pella, Inc., Redding, CA). For fluorescence microscopy, the M3/18 cells transiently expressing DRM-labeled fusion proteins were fixed and mounted as described above. GFP-tagged Dad1 stably expressed in M3/18 cells or microtubules decorated with the antibodies were visualized using the FITC filter set. The DRM-tagged proteins were visualized using a Texas Red filter set. Slides were examined under the microscope using Plan-Apochromat 100×/1.4 N.A. DIC oil-immersed lenses (Carl Zeiss). The images were obtained at scan-zoom 1 with the line averaging set at '4' and the pinhole completely open. The channel representing Alexa Fluor-633 staining was colored green. Collected images were exported into JPEG format, assembled into panels and annotated using Abode Photoshop 7.

Fluorescence recovery after photobleaching

For fluorescence recovery after photobleaching (FRAP) experiments, M3/18 cells were seeded and grown overnight at 39.5°C on glass-bottom No. 0 35-mm tissue culture dishes (MatTek) in complete growth medium. In FRAP experiments studying the effects of the drugs on the lateral mobility of the TCs, M3/18 cells were treated with cycloheximide (CHX, 100 μM for 30 minutes), NaCl (150 mM for 10 minutes), latrunculin B (10 μM for 2 hours); nocodazole (33 μM for 4 hours), puromycin (100 μM for 30 minutes) or taxol (5 μM for 4 hours) at 39.5°C just before performing the experiments. If two drugs were used, the drug requiring longer incubation was added first. If needed, the cells were transfected with recombinant plasmid DNA encoding DRM-tagged fusion proteins and left to grow overnight at 10% CO_2 and 39.5°C. Since there is no overlap in the excitation and emission spectra of DRM and GFP, the FRAP experiments can be performed on the GFP-tagged proteins in the presence of DRM-tagged fusion proteins. Photobleaching, FRAP data collection and analysis were done as previously described (Nikonov et al., 2002) with one exception – all experiments were done using the environmental chamber with heated stage purchased from Carl Zeiss, Inc. The temperature in the chamber was set to 39.5°C and moist circulating air was supplemented with 10% CO_2. Images were collected using Neofluar 40×/1.2 N.A. water objective. To collect fluorescence from the entire depth of the cell, the pinhole was wide-opened. All images were collected on an 8-bit PMT (Carl Zeiss, Jena, Germany). No saturated images were used for FRAP analysis. FRAP experiments on BHK-21 cells expressing LBR-GFP were done as described for M3/18 cells.

Statistical analysis of FRAP data

The calculated values of the diffusion coefficients (D_{eff}) were were listed according to experimental conditions in a Microsoft Office Excel 2003 worksheet. Data were subjected to the two-sample *t*-test, where variances were assumed unequal and alpha was set to 0.05. The test was performed pair-wise (control versus experimental group), hypothesizing that there is no difference between the two groups analyzed. The calculated means of D_{eff} and probabilities, $P(T \leq t)$, are given in the tables. The closer the $P(T \leq t)$ values are to 1, the more similar are the two tested groups. Standard deviation (s.d.) was calculated using the build-in function stdev of MS-Excel.

Calculation of the sizes of translocon assemblies

The radii of the TC assemblies were calculated according to Edidin and co-workers (Marguet et al., 1999). The equation used takes into consideration only friction between transmembrane domains the TC and the lipid bilayer of ER membranes. It does not consider possible interactions with other protein complexes or cytoskeletal elements. D_{eff} for LBR-GFP and the theoretical radius of a single transmembrane domain (TMD) were used in these calculations. The calculated radii were converted into the area values. The number of the TCs that a calculated area potentially holds was established by dividing the value of the area occupied by the TC assemblies by the value of the area occupied by an individual TC.

The area occupied by an individual TC was calculated using the following assumptions: From published data (Johnson and van Waes, 1999; Nilsson et al., 2003), we estimated that a single translocon complex (TC) has at least 23 subunits containing 78 transmembrane domains (TMD). The mammalian OST was assumed to have six subunits: ribophorin I (67 kDa, 1 TMD, GenBank accession number P04843), ribophorin II (63 kDa, 1 TMD, GenBank accession number P04844), OST48 (48 kDa, 1 TMD, GenBank accession number P39656), Dad1 (10 kDa, 2 TMD, GenBank accession number P61803), STT3A or STT3B (85 kDa, 13 TMD, GenBank accession number Q8TCJ2), and N33 or IAP (34 kDa, 4 TMD, GenBank accession number Q9H0U3). Therefore, the OST should have a molecular mass of at least 307 kDa and 22 TMD. Yeast OST has two additional subunits, OST4p (4 kDa, 1 TMD, GenBank accession number Q99380) and OST5p (9.5 kDa, 2 TMD, GenBank accession number Q92316). However, no mammalian homologs have so far been described and we did not include them in our calculations. In addition to the OST, the TC contains three sets of the Sec61p complex. One Sec61p complex consist of three subunits – α, β and γ (80 kDa and 12 TMD in total), three sets would have a molecular mass of 240 kDa and 36 TMD. Other components of the TC are TRAM (40 kDa, 8 TMD), the α and β subunits of the SRP receptor (100 kDa, 2 TMD in total), two subunits of signal peptidase (100 kDa, 2 TMD in total),

and TRAP (90 kDa, 4 TMD). All subunits of the TC would have a molecular mass of about 950 kDa containing 78 TMD.

This work was supported by National Science Foundation grant 0349142.

References

Adelman, M. R., Sabatini, D. D. and Blobel, G. (1973). Ribosome-membrane interaction. Nondestructive disassembly of rat liver rough microsomes into ribosomal and membranous components. *J. Cell Biol.* **56**, 206-229.

Amarilio, R., Ramachandran, S., Sabanay, H. and Lev, S. (2005). Differential regulation of endoplasmic reticulum structure through VAP-Nir protein interaction. *J. Biol. Chem.* **280**, 5934-5944.

Andrade, J., Zhao, H., Titus, B., Timm Pearce, S. and Barroso, M. (2004). The EF-hand Ca2+-binding protein p22 plays a role in microtubule and endoplasmic reticulum organization and dynamics with distinct Ca2+-binding requirements. *Mol. Biol. Cell* **15**, 481-496.

Bierer, B. E., Herrmann, S. H., Brown, C. S., Burakoff, S. J. and Golan, D. E. (1987). Lateral mobility of class I histocompatibility antigens in B lymphoblastoid cell membranes: modulation by cross-linking and effect of cell density. *J. Cell Biol.* **105**, 1147-1152.

Borgese, N., Francolini, M. and Snapp, E. (2006). Endoplasmic reticulum architecture: structures in flux. *Curr. Opin. Cell Biol.* **18**, 358-364.

Christensen, A. K. and Bourne, C. M. (1999). Shape of large bound polysomes in cultured fibroblasts and thyroid epithelial cells. *Anat. Rec.* **255**, 116-129.

Christensen, A. K., Kahn, L. E. and Bourne, C. M. (1987). Circular polysomes predominate on the rough endoplasmic reticulum of somatotropes and mammotropes in the rat anterior pituitary. *Am. J. Anat.* **178**, 1-10.

Clemons, W. M., Jr, Menetret, J. F., Akey, C. W. and Rapoport, T. A. (2004). Structural insight into the protein translocation channel. *Curr. Opin. Struct. Biol.* **14**, 390-396.

Dabora, S. L. and Sheetz, M. P. (1988). The microtubule-dependent formation of a tubulovesicular network with characteristics of the ER from cultured cell extracts. *Cell* **54**, 27-35.

Dreier, L. and Rapoport, T. A. (2000). In vitro formation of the endoplasmic reticulum occurs independently of microtubules by a controlled fusion reaction. *J. Cell Biol.* **148**, 883-898.

Ellenberg, J., Siggia, E. D., Moreira, J. E., Smith, C. L., Presley, J. F., Worman, H. J. and Lippincott-Schwartz, J. (1997). Nuclear membrane dynamics and reassembly in living cells: targeting of an inner nuclear membrane protein in interphase and mitosis. *J. Cell Biol.* **138**, 1193-1206.

Evans, K. J., Gomes, E. R., Reisenweber, S. M., Gundersen, G. G. and Lauring, B. P. (2005). Linking axonal degeneration to microtubule remodeling by Spastin-mediated microtubule severing. *J. Cell Biol.* **168**, 599-606.

Farah, C. A., Liazoghli, D., Perreault, S., Desjardins, M., Guimont, A., Anton, A., Lauzon, M., Kreibich, G., Paiement, J. and Leclerc, N. (2005). Interaction of microtubule-associated protein-2 and p63: a new link between microtubules and rough endoplasmic reticulum membranes in neurons. *J. Biol. Chem.* **280**, 9439-9449.

Fawcett, D. W. (1966). *An Atlas of Fine Structure. The Cell, its Organells and Inclusions*. Philadelphia, London: W. B. Saunders.

Gilmore, R. (1993). Protein translocation across the endoplasmic reticulum: a tunnel with toll booths at entry and exit. *Cell* **75**, 589-592.

Jacobson, K., Sheets, E. D. and Simson, R. (1995). Revisiting the fluid mosaic model of membranes. *Science* **268**, 1441-1442.

Johnson, A. E. and van Waes, M. A. (1999). The translocon: a dynamic gateway at the ER membrane. *Annu. Rev. Cell Dev. Biol.* **15**, 799-842.

Jordan, M. A., Toso, R. J., Thrower, D. and Wilson, L. (1993). Mechanism of mitotic block and inhibition of cell proliferation by taxol at low concentrations. *Proc. Natl. Acad. Sci. USA* **90**, 9552-9556.

Klopfenstein, D. R., Kappeler, F. and Hauri, H. P. (1998). A novel direct interaction of endoplasmic reticulum with microtubules. *EMBO J.* **17**, 6168-6177.

Klopfenstein, D. R., Klumperman, J., Lustig, A., Kammerer, R. A., Oorschot, V. and Hauri, H. P. (2001). Subdomain-specific localization of CLIMP-63 (p63) in the endoplasmic reticulum is mediated by its luminal alpha-helical segment. *J. Cell Biol.* **153**, 1287-1300.

Kreibich, G., Ulrich, B. L. and Sabatini, D. D. (1978). Proteins of rough microsomal membranes related to ribosome binding. I. Identification of ribophorins I and II, membrane proteins characteristics of rough microsomes. *J. Cell Biol.* **77**, 464-487.

Lippincott-Schwartz, J., Presley, J. F., Zaal, K. J., Hirschberg, K., Miller, C. D. and Ellenberg, J. (1999). Monitoring the dynamics and mobility of membrane proteins tagged with green fluorescent protein. *Methods Cell Biol.* **58**, 261-281.

Lippincott-Schwartz, J., Snapp, E. and Kenworthy, A. (2001). Studying protein dynamics in living cells. *Nat. Rev. Mol. Cell Biol.* **2**, 444-456.

Marcantonio, E. E., Grebenau, R. C., Sabatini, D. D. and Kreibich, G. (1982). Identification of ribophorins in rough microsomal membranes from different organs of several species. *Eur. J. Biochem.* **124**, 217-222.

Marguet, D., Spiliotis, E. T., Pentcheva, T., Lebowitz, M., Schneck, J. and Edidin, M. (1999). Lateral diffusion of GFP-tagged H2Ld molecules and of GFP-TAP1 reports on the assembly and retention of these molecules in the endoplasmic reticulum. *Immunity* **11**, 231-240.

Marsh, B. J., Mastronarde, D. N., Buttle, K. F., Howell, K. E. and McIntosh, J. R. (2001). Organellar relationships in the Golgi region of the pancreatic beta cell line, HIT-T15, visualized by high resolution electron tomography. *Proc. Natl. Acad. Sci. USA* **98**, 2399-2406.

McCallum, C. D., Do, H., Johnson, A. E. and Frydman, J. (2000). The interaction of the chaperonin tailless complex polypeptide 1 (TCP1) ring complex (TRiC) with ribosome-bound nascent chains examined using photo-cross-linking. *J. Cell Biol.* **149**, 591-602.

Menetret, J. F., Neuhof, A., Morgan, D. G., Plath, K., Radermacher, M., Rapoport, T. A. and Akey, C. W. (2000). The structure of ribosome-channel complexes engaged in protein translocation. *Mol. Cell* **6**, 1219-1232.

Nikonov, A. V., Korolev, E. V., Snigirevskaia, E. S., Brudnaia, M. S., Komissarchik, I., Ivanov, P. I. and Borkhsenius, S. N. (1992). [Tubular structures in Mycoplasma gallisepticum and the localization of a tubulin-like protein]. *Tsitologiia* **34**, 31-38.

Nikonov, A. V., Snapp, E., Lippincott-Schwartz, J. and Kreibich, G. (2002). Active translocon complexes labeled with GFP-Dad1 diffuse slowly as large polysome arrays in the endoplasmic reticulum. *J. Cell Biol.* **158**, 497-506.

Nilsson, I., Kelleher, D. J., Miao, Y., Shao, Y., Kreibich, G., Gilmore, R., von Heijne, G. and Johnson, A. E. (2003). Photocross-linking of nascent chains to the STT3 subunit of the oligosaccharyltransferase complex. *J. Cell Biol.* **161**, 715-725.

Ogura, T. and Wilkinson, A. J. (2001). AAA+ superfamily ATPases: common structure–diverse function. *Genes Cells* **6**, 575-597.

Potter, M. D. and Nicchitta, C. V. (2000a). Regulation of ribosome detachment from the mammalian endoplasmic reticulum membrane. *J. Biol. Chem.* **275**, 33828-33835.

Potter, M. D. and Nicchitta, C. V. (2000b). Ribosome-independent regulation of translocon composition and Sec61alpha conformation. *J. Biol. Chem.* **275**, 2037-2045.

Rajasekaran, A. K., Morimoto, T., Hanzel, D. K., Rodriguez-Boulan, E. and Kreibich, G. (1993). Structural reorganization of the rough endoplasmic reticulum without size expansion accounts for dexamethasone-induced secretory activity in AR42J cells. *J. Cell Sci.* **105**, 333-345.

Rapoport, T. A., Jungnickel, B. and Kutay, U. (1996). Protein transport across the eukaryotic endoplasmic reticulum and bacterial inner membranes. *Annu. Rev. Biochem.* **65**, 271-303.

Rapoport, T. A., Goder, V., Heinrich, S. U. and Matlack, K. E. (2004). Membrane-protein integration and the role of the translocation channel. *Trends Cell Biol.* **14**, 568-575.

Rennison, M. E., Handel, S. E., Wilde, C. J. and Burgoyne, R. D. (1992). Investigation of the role of microtubules in protein secretion from lactating mouse mammary epithelial cells. *J. Cell Sci.* **102**, 239-247.

Sabatini, D. D. and Kreibich, G. (1976). Functional Specialization of membrane-bound ribosomes in eukaryotic cells. In *The Enzymes of Biological Membranes. Biosynthesis of Cell Components*. Vol. 2 (ed. A. Martonosi), pp. 531-579. New York, London: Plenum Press.

Sabatini, D. D. and Adesnik, M. (1995). The biogenesis of membranes and organelles. In *The Metabolic Basis of Inherited Disease* (ed. C. R. Scriver, A. L. Beaudet, W. S. Sly and D. Valle), pp. 459-553. New York: McGraw-Hill.

Saborio, J. L., Pong, S. S. and Koch, G. (1974). Selective and reversible inhibition of initiation of protein synthesis in mammalian cells. *J. Mol. Biol.* **85**, 195-211.

Schiff, P. B. and Horwitz, S. B. (1980). Taxol stabilizes microtubules in mouse fibroblast cells. *Proc. Natl. Acad. Sci. USA* **77**, 1561-1565.

Schiff, P. B., Fant, J. and Horwitz, S. B. (1979). Promotion of microtubule assembly in vitro by taxol. *Nature* **277**, 665-667.

Schweizer, A., Ericsson, M., Bachi, T., Griffiths, G. and Hauri, H. P. (1993a). Characterization of a novel 63 kDa membrane protein. Implications for the organization of the ER-to-Golgi pathway. *J. Cell Sci.* **104**, 671-683.

Schweizer, A., Peter, F., Nguyen Van, P., Soling, H. D. and Hauri, H. P. (1993b). A luminal calcium-binding protein with a KDEL endoplasmic reticulum retention motif in the ER-Golgi intermediate compartment. *Eur. J. Cell Biol.* **60**, 366-370.

Schweizer, A., Rohrer, J., Jeno, P., DeMaio, A., Buchman, T. G. and Hauri, H. P. (1993c). A reversibly palmitoylated resident protein (p63) of an ER-Golgi intermediate compartment is related to a circulatory shock resuscitation protein. *J. Cell Sci.* **104**, 685-694.

Schweizer, A., Rohrer, J., Slot, J. W., Geuze, H. J. and Kornfeld, S. (1995). Reassessment of the subcellular localization of p63. *J. Cell Sci.* **108**, 2477-2485.

Seiser, R. M. and Nicchitta, C. V. (2000). The fate of membrane-bound ribosomes following the termination of protein synthesis. *J. Biol. Chem.* **275**, 33820-33827.

Shibata, Y., Voeltz, G. K. and Rapoport, T. A. (2006). Rough sheets and smooth tubules. *Cell* **126**, 435-439.

Singer, S. J. and Nicolson, G. L. (1972). The fluid mosaic model of the structure of cell membranes. *Science* **175**, 720-731.

Spector, I., Shochet, N. R., Blasberger, D. and Kashman, Y. (1989). Latrunculins – novel marine macrolides that disrupt microfilament organization and affect cell growth: I. Comparison with cytochalasin D. *Cell Motil. Cytoskeleton* **13**, 127-144.

Storrie, B., White, J., Rottger, S., Stelzer, E. H., Suganuma, T. and Nilsson, T. (1998). Recycling of golgi-resident glycosyltransferases through the ER reveals a novel pathway and provides an explanation for nocodazole-induced Golgi scattering. *J. Cell Biol.* **143**, 1505-1521.

Terasaki, M., Chen, L. B. and Fujiwara, K. (1986). Microtubules and the endoplasmic reticulum are highly interdependent structures. *J. Cell Biol.* **103**, 1557-1568.

Vaz, W. L., Criado, M., Madeira, V. M., Schoellmann, G. and Jovin, T. M. (1982). Size dependence of the translational diffusion of large integral membrane proteins in liquid-crystalline phase lipid bilayers. A study using fluorescence recovery after photobleaching. *Biochemistry* **21**, 5608-5612.

Vazquez, D. (1974). Inhibitors of protein synthesis. *FEBS Lett.* **40**, S63-S84.
Vedrenne, C., Klopfenstein, D. R. and Hauri, H. P. (2005). Phosphorylation controls CLIMP-63-mediated anchoring of the endoplasmic reticulum to microtubules. *Mol. Biol. Cell* **16**, 1928-1937.
Voeltz, G. K., Rolls, M. M. and Rapoport, T. A. (2002). Structural organization of the endoplasmic reticulum. *EMBO Rep.* **3**, 944-950.
Wakatsuki, T., Schwab, B., Thompson, N. C. and Elson, E. L. (2001). Effects of cytochalasin D and latrunculin B on mechanical properties of cells. *J. Cell Sci.* **114**, 1025-1036.
Walter, P. and Johnson, A. E. (1994). Signal sequence recognition and protein targeting to the endoplasmic reticulum membrane. *Annu. Rev. Cell Biol.* **10**, 87-119.
Wengler, G. (1972). Medium hypertonicity and polyribosome structure in Hela cells. The influence of hypertonicity of the growth medium on polyribosomes in Hela cells. *Eur. J. Biochem.* **27**, 162-173.
Wiedmann, B., Sakai, H., Davis, T. A. and Wiedmann, M. (1994). A protein complex required for signal-sequence-specific sorting and translocation. *Nature* **370**, 434-440.
Yvon, A. M., Wadsworth, P. and Jordan, M. A. (1999). Taxol suppresses dynamics of individual microtubules in living human tumor cells. *Mol. Biol. Cell* **10**, 947-959.
Zhang, F., Crise, B., Su, B., Hou, Y., Rose, J. K., Bothwell, A. and Jacobson, K. (1991). Lateral diffusion of membrane-spanning and glycosylphosphatidylinositol-linked proteins: toward establishing rules governing the lateral mobility of membrane proteins. *J. Cell Biol.* **115**, 75-84.